PHYSICAL REVIEW A **71**, 020701(R) (2005)

Configuration-interaction-induced dynamic spin polarization of the $Ar^*(2p^{-1}_{1/2,3/2}4s_{1/2})_{J=1}$ resonant Auger decay

B. Lohmann,[1,2,*] B. Langer,[3] G. Snell,[4,†] U. Kleiman,[2,‡] S. Canton,[4,†] M. Martins,[5] U. Becker,[2] and N. Berrah[4]

[1]*Institut für Theoretische Physik, Westfälische Wilhelms-Universität Münster, Wilhelm-Klemm-Strasse 9, D-48149 Münster, Germany*

[2]*Fritz-Haber-Institut der Max-Planck-Gesellschaft, Faradayweg 4-6, D-14195 Berlin/Dahlem, Germany*

[3]*Max-Born-Institut für Nichtlineare Optik und Kurzzeitspektroskopie, Max-Born-Strasse 2A, D-12489 Berlin, Germany*

[4]*Department of Physics, Western Michigan University, Kalamazoo, Michigan 49008, USA*

[5]*Institut für Experimentalphysik, Universität Hamburg, Luruper Chaussee 149, D-22761 Hamburg, Germany*

(Received 7 April 2004; published 9 February 2005; corrected 17 February 2005)

Spin-resolved measurements of the $Ar^*(2p^{-1}_{1/2,3/2}4s_{1/2})_{J=1}$ resonantly excited $L_{2,3}M_{2,3}M_{2,3}$ Auger decay have been performed. The low resolution Auger spectrum, which due to cancellation between different multiplet components should exhibit virtually zero dynamic spin polarization, reveals an unexpected nonvanishing polarization effect. Calculations within a relativistic distorted wave approximation explain this effect as configuration-interaction (CI) induced. The CI generates experimentally unresolved fine structure components with low and high total angular momentum, giving rise to asymmetric cases where the high J part of certain multiplets is suppressed by internal selection rules for diagram lines. In this case, only the low J components survive with no partner for spin-polarization cancellation.

DOI: 10.1103/PhysRevA.71.020701 PACS number(s): 32.80.Hd, 32.80.Rm, 31.25.Jf, 31.15.Ar

Spin polarization of photoelectrons and Auger electrons, the most sensitive probe of the magnetic properties of matter, is directly related to the generally anisotropic *e*-*e* correlation during the electron emission. In particular, spin polarization manifests itself via two physically different effects. The electrons may be spin polarized due to polarization transfer by circularly polarized light, but also due to the interference between different partial waves emitted by linearly polarized light. The transferred spin polarization (TSP) is generally large because of the asymmetric m-sublevel population [1–7] generated by the circularly polarized light. This is not the case for the dynamic spin polarization (DSP) induced by linearly or even unpolarized light. The latter is related to the fact that photons are generally aligned due to their transversal character. The DSP shows higher values only if certain conditions concerning the number of contributing partial waves and their relative phase shifts are fulfilled [6,8]. Particularly, a fully resolved fine structure has been hitherto recognized as a prerequisite for a nonvanishing DSP in a nonrelativistic approximation. We report on the first experimental analysis and theoretical interpretation of both types of spin polarization in one Auger spectrum, here the prominent *LMM* spectrum of Ar.

Resonant Auger decay from 2p-excited argon atoms is a showcase for large TSP but vanishing DSP. The first may be understood from the close similarity with d-shell photoionization, particularly the case with f-wave suppression. The reason for the very small DSP is twofold: on one hand it is in accordance with recently derived propensity rules [8], showing that for most resonant Auger transitions, due to parity arguments, their partial waves are emitted with equal orbital angular momentum, hence, having very small phase differences that, in turn, diminishes the DSP. This vanishing relativistic phase shift situation is also known from photoionization [4]. Our measurements performed at the Advanced Light Source (ALS) in Berkeley and our calculations obtained within a relativistic distorted wave approximation (RDWA) corroborate these assumptions. On the other hand, the different fine structure components tend to cancel their spin polarization with respect to each other due to the requirement of vanishing DSP for the whole multiplet in pure *LS* coupling. This is because all spin polarization effects are mediated via the spin orbit interaction [9–13]. As a consequence, nonresolved fine structure components should exhibit almost no measurable DSP. Therefore, virtually no DSP is expected for a light element such as argon, i.e., the resonant $L_{2,3}M_{2,3}M_{2,3}$ Auger spectrum following the $Ar^*(2p^{-1}_{1/2,3/2}4s_{1/2})_{J=1}$ excitation with linearly polarized light. However, the experimental low resolution spectra exhibit measurable DSP, at least for one unresolved group of lines. We have been able to explain this unexpected occurrence of DSP by strong configuration interaction (CI) in the final ionic state. Our work represents a combined experimental and theoretical demonstration of a mechanism that gives rise to the DSP of unresolved Auger lines.

Defining the reaction plane by the incoming synchrotron beam axis and the direction of the Auger emission, both DSP and TSP can be related to the in-reaction plane component of the spin polarization vector perpendicular to the direction of Auger emission [14]. Describing the resonant Auger transitions in the well-observed two-step model [15], the DSP and TSP factorize into a set of alignment and orientation param-

*Author to whom correspondence should be addressed. Electronic address: lohmanb@uni-muenster.de

†Present address: Advanced Light Source, Lawrence Berkeley National Laboratory, Berkeley, CA 94720, USA.

‡Present address: Auburn University, Department of Physics, Auburn, AL 36849, USA.

eters containing solely the dynamics of the primary excitation, and angular distribution and spin polarization parameters describing the dynamics of the resonant Auger decay.

In our case, measuring the DSP after photoexcitation with a linearly polarized photon beam yields the advantage of a maximum alignment $\mathcal{A}_{20}=-\sqrt{2}$ [16] in the polarization reference system, and the component of the spin polarization vector may be written as (see [14])

$$P_{dyn}(\theta,\phi)=\frac{-3\xi_2\sin(2\phi)\sin\theta}{\sqrt{2}+\alpha_2\left[P_2(\cos\theta)-\frac{3}{2}\cos(2\phi)\sin^2\theta\right]}, \quad (1)$$

where $P_2(\cos\theta)$ denotes the second Legendre polynomial and θ is the angle between the synchrotron beam axis and the direction of the Auger emission while ϕ gives the angle between the reaction plane and the oscillation plane of the electric field vector, which coincides with the synchrotron storage ring plane. ξ_2 and α_2 are the dynamic spin polarization and angular anisotropy parameters, respectively. The spin-polarization parameter ξ_2 has not been uniquely defined in the literature, e.g., [6,8–10]. We use here the expression given by Lohmann [8], which is based on a somewhat different separation between the spin polarization parameter and the angular part. An expression for α_2 is given in [17]. These parameters consist of coherent sums over products of partial wave Auger transition amplitudes multiplied by their corresponding phase shift differences and related Clebsch-Gordan and Wigner coefficients.

Our experiment has been performed in the emission reference system under the fixed geometry $\theta_{exp}=90°$ and $\phi_{exp}=135°$. Inserting θ_{exp},ϕ_{exp} into Eq. (1) we obtain the DSP as

$$P_{dyn}(\theta_{exp},\phi_{exp})=(6\xi_2)/(2\sqrt{2}-\alpha_2). \quad (2)$$

Similarly, for a fully circularly polarized photon beam, the TSP can be related to the same component of the spin polarization vector which yields

$$p_{trans}(\theta)=(\sqrt{3}\xi_1\sin\theta)/[\sqrt{2}+\alpha_2 P_2(\cos\theta)], \quad (3)$$

where ξ_1 refers to as the transferred spin-polarization parameter [5]. The TSP becomes independent of the azimuthal angle ϕ because the combined photonic and target system, where the latter has been assumed as unpolarized, is axially symmetric with respect to the synchrotron beam axis.

Thus, the TSP can be measured under the same solid angle as the DSP, i.e., $\theta_{exp}=90°$, while ϕ_{exp} becomes redundant, which yields

$$p_{trans}(\theta_{exp})=(2\sqrt{3}\xi_1)/(2\sqrt{2}-\alpha_2). \quad (4)$$

Our numerical data have been obtained employing a relativistic distorted wave approximation (RDWA). Here, the bound state wave functions of the excited intermediate and the ionized final state of the atom are constructed using the multiconfigurational Dirac-Fock (MCDF) computer code of Grant *et al.* [18]. Intermediate coupling has been taken into account where the mixing coefficients have been calculated applying the average level calculation mode (see [18]). The calculation of the Auger transition matrix elements has been done applying a relaxed orbital method. Thus, the bound electron wave functions of the intermediate state are calculated in the field of the excited atom, whereas the bound electron wave functions of the final state are calculated in the field of the singly ionized atom.

The atomic state function (ASF) of the intermediate excited and the singly ionized final state have been constructed as linear combinations of configuration state functions (CSF)

$$|\psi_\alpha(PJM)\rangle=\sum_{r=1}^{n_c}c_r(\alpha)|\gamma_r PJM\rangle. \quad (5)$$

The configuration states $|\gamma_r PJM\rangle$ are constructed from antisymmetrized products of Dirac orbitals, which are eigenstates of the total (one-electron) angular momentum and parity. The label γ_r distinguishes the occupation of the different subshells and angular coupling schemes (see Grant [19] for further details). n_c is the number of CSF included in the expansion and $c_r(\alpha)$, $r=1,\ldots,n_c$, are the configuration mixing coefficients for the state α.

The intermediate excited state has been generated as a linear combination from the five possible jj-coupled $Ar^*(2p^{-1}_{1/2,3/2}4s_{1/2})_{J=1}$ and $Ar^*(2p^{-1}_{1/2,3/2}3d_{3/2,5/2})_{J=1}$ CSF. We find the $Ar^*(2p^{-1}_{3/2}4s_{1/2})_{J=1}$ and $Ar^*(2p^{-1}_{1/2}4s_{1/2})_{J=1}$ ASF as almost pure states.

Two calculations have been performed for the final ionic state. In calculation (a) a basis set of eight CSF has been used to generate the final state ASF from the possible linear combinations of the $Ar^+(3p^{-2}_{1/2,3/2}4s_{1/2})$ jj-coupled states (8 CSF-CI). Since this approach has not been able to reveal all lines of the spectrum [20,21] our calculation (b) accounts for all jj-coupled $Ar^+(3p^{-2}_{1/2,3/2}3d_{3/2,5/2})$ CSF, too. Thus, a basis of 36 CSF has been used to generate the final state ASF (36 CSF-CI).

Eventually, the continuum wave function of the Auger electron is evaluated by solving the Dirac equation with an intermediate coupling potential where electron exchange with the continuum has been taken into account. The intermediate coupling potential is constructed from the mixed CSF of the final ionic state. Thereby we take into account, that the ejected electron moves within the field of the residual ion. With this, the Auger transition matrix elements are obtained for calculating the relevant angular anisotropy and spin polarization parameters, respectively. Note, that both are not functions of the transition matrix elements, only but explicitly depend on the scattering phases. Further information may be found in [5,7].

We have measured the spin-resolved electron spectra of the Ar $2p_{3/2}\rightarrow 4s_{1/2}$ and Ar $2p_{1/2}\rightarrow 4s_{1/2}$ autoionization resonances. The experiment has been performed at the ALS operating in two-bunch mode, utilizing the elliptically polarizing undulator (EPU) at Beamline 4.0.2 [22]. The EPU was set to deliver 100% circularly or linearly polarized light at all used photon energies. Electron energy analysis has been performed using a time-of-flight (TOF) spectrometer, collecting electrons emitted at 45° with respect to the storage ring plane [27] in the direction perpendicular to the photon propagation. A spherical Mott polarimeter of the Rice type, operated at 25 kV, mounted at the end of the TOF has been used to carry out the electron spin polarization analysis [23–25]. The geometry of the experiment has been chosen to measure the

polarization of the spin components of the electrons along the photon propagation direction [26]. The instrumental asymmetries of the Mott polarimeter have been eliminated by reversing the helicity in the case of circularly polarized light and switching the polarization from horizontal to vertical in the case of linearly polarized light. The transferred and dynamic electron spin polarizations, corresponding to $p_{trans}(\theta_{exp}=90°)$ and $p_{dyn}(\theta_{exp}=90°, \phi_{exp}=135°)$, respectively, can be calculated from the four measured intensities I_1^+, I_1^-, I_2^+, and I_2^- as follows:

$$p_{trans,dyn}(\theta_{exp},\phi_{exp}) = \frac{1}{S_{eff}} \frac{\sqrt{I_1^+ I_2^-} - \sqrt{I_1^- I_2^+}}{\sqrt{I_1^+ I_2^-} + \sqrt{I_1^- I_2^+}}. \quad (6)$$

The lower index denotes the multichannel plates (MCP) of the Mott detector and the upper index stands for the helicity, respectively the horizontal or vertical polarization of the light. S_{eff} describes the analyzing power of the polarimeter (the effective Sherman function), which has been determined

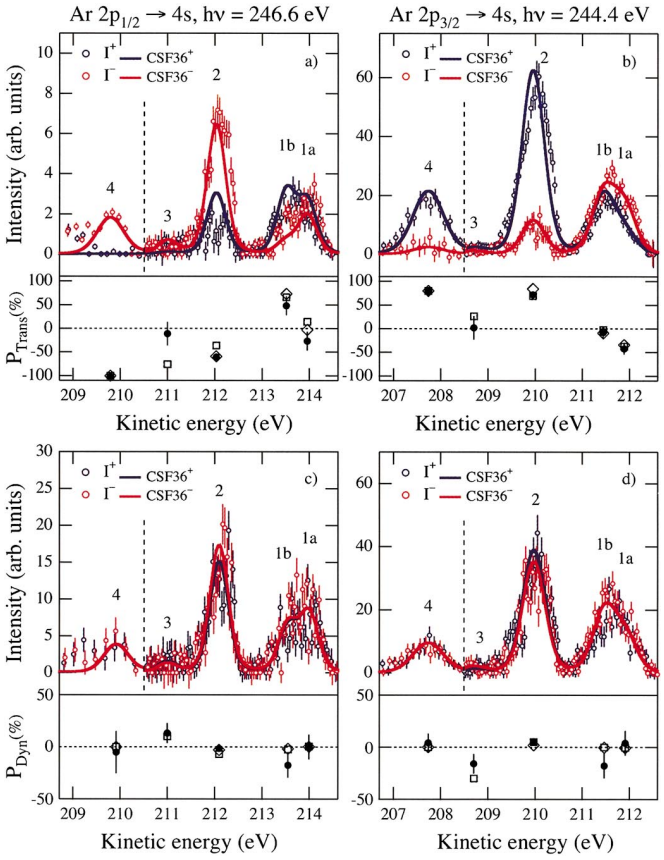

FIG. 1. (Color) Spin-resolved spectrum for the TSP [(a) and (b)] and DSP [(c) and (d)] for excitation with circularly and linearly polarized light, respectively. Full curves: 36 CSF-CI. Circles with errorbars: experimental data. Blue: partial intensities for spin up (I^+). Red: partial intensities for spin down (I^-). The degree of DSP and TSP for the unresolved group of lines is shown in the chart underneath. Open diamonds: 8 CSF-CI. Open squares: 36 CSF-CI. Filled circles: experimental data. The dashed lines in all figures separate spectra taken with different resolutions and, hence, retardation voltage.

TABLE I. The calculated degree of dynamic, $p_{dyn}(\theta_{exp},\phi_{exp})$, and transferred, $p_{trans}(\theta_{exp})$, spin polarization is given. Note, that transitions to fine structure terms with $J \geqslant 7/2$ are suppressed due to J-dependent selection rules. (a) Our tentative assignment of the observed and calculated peaks (36 CSF) of the unresolved LSJ fine structure terms. (b) Peak numbers are as assigned in the experimental spectrum.

$Ar^*L_{2,3}M_{2,3}M_{2,3}$ Final states	No.	$2p_{3/2} \rightarrow 4s$ Spin polarization %		$2p_{1/2} \rightarrow 4s$	
(a)	(b)	p_{dyn}	p_{trans}	p_{dyn}	p_{trans}
$\|(3p^2[^3P]4s)^4P_{1/2,\ldots,5/2}\rangle$ $\|(3p^2[^3P]3d)^4D_{1/2,\ldots,7/2}\rangle$	1a	−0.30	−42.51	0.49	8.53
$\|(3p^2[^3P]4s)^2P_{1/2,3/2}\rangle$	1b	−0.06	−2.57	−2.38	66.31
$\|(3p^2[^3P]3d)^2P_{1/2,3/2}\rangle$ $\|(3p^2[^3P]3d)^4P_{1/2,\ldots,5/2}\rangle$ $\|(3p^2[^1D]4s)^2D_{3/2,5/2}\rangle$ $\|(3p^2[^3P]3d)^2F_{5/2,7/2}\rangle$ $\|(3p^2[^3P]3d)^4D_{3/2,5/2}\rangle$	2	4.42	69.50	−4.07	−41.36
$\|(3p^2[^1D]3d)^2F_{5/2,7/2}\rangle$ $\|(3p^2[^1D]3d)^2S_{1/2}\rangle$	3	−30.29	25.62	10.14	−75.88
$\|(3p^2[^1S]4s)^2S_{1/2,}\rangle$	4	0.02	79.56	−0.02	−99.98

to be $S_{eff}=0.13(3)$. Measurement of the DSP and TSP has been achieved arranging MCP_1 and MCP_2 perpendicular to the reaction plane using linearly and circularly polarized light for the DSP and TSP, respectively. A more detailed description of the experiment and the analysis is given by Snell *et al.* [26].

Using Eqs. (2) and (4) we have been able to plot the spin-up and spin-down partial intensities of the spectrum. Our results are shown in Figs. 1(a) and 1(b) for the spin-resolved spectrum for the TSP and in Figs. 1(c) and 1(d) for the spin-resolved DSP spectrum of the $L_{2,3}M_{2,3}M_{2,3}$ Auger decay for the excited intermediate argon $(2p_{1/2}^{-1}4s_{1/2})_{J=1}$ and $(2p_{3/2}^{-1}4s_{1/2})_{J=1}$ states, respectively, along with the results of the extended 36 CSF calculation.

The spectrum has been generated assuming a Lorentz profile with a full width at half maximum (FWHM)=0.1 eV for the Auger lines folded with the appropriate Gaussian line shape. The partial intensities of the 36 CSF-CI represent the calculated spin polarizations, as shown in Table I, but normalized to the experimental total intensities and shifted by an energy offset. A bar diagram underneath of the partial intensities shows the integral values of the spin polarization for the most prominent Auger lines. The filled bars represent the experimental values, whereas the two open bars refer to our results for the eight CSF and the extended 36 CSF calculations, respectively. Besides the generation of new lines at lower kinetic energies, of which only line 3 is shown in Fig. 1 and Table I, the comparison reveals an unexpected difference between the two types of spin polarization, transferred and dynamic; whereas for the TSP there is little improvement between the two calculations, only—the eight CSF-CI repro-

duces the experimental data already very well, particularly for the $3p_{3/2}$ excitation—the corresponding results for the DSP differ qualitatively. In this case, the eight CSF-CI yield a vanishing spin polarization over the whole spectrum. Reasonable agreement with the experiment, showing nonvanishing spin polarization for some lines (2, 3), can be achieved only by employing the extended 36 CSF-CI. Inspecting more closely the different transitions contributing to the spin-polarized part of the spectrum reveals that the CI with 36 CSF, in contrast to the eight CSF-CI, generates unresolved fine structure components with low and high total angular momentum as shown in Table I. The 36 CSF-CI produces J components that correspond in a tentative LSJ coupling scheme to ${}^2L_{J,J'}$ states with $L \geqslant 3$ and $J, J' \geqslant 5/2, 7/2$. These virtual fine structure components however, require nondiagram lines in the form of Auger satellites in order to populate the high J part. Stressing the picture of Auger decay as a two-electron transition, the nondiagram lines are normally an order of magnitude lower than the corresponding diagram lines, similar to the situation in photoionization concerning main and satellite lines. Consequently, such a situation of fine structure multiplets with a mixed diagram-nondiagram character gives rise to the possibility of asymmetric cases where the high J part of certain multiplets is suppressed due to J-dependent selection rules. Therefore, only the low J components survive with no partner for polarization cancellation. However, both the statistics of the experimental data as well as the number of configurations included in the CI calculations requires further improvements in order to quantify the observed effect in more detail.

In conclusion, our spin-resolved, low-resolution measurements of the resonant Auger electrons from $2p$-excited Ar by linearly polarized light has revealed a measurable DSP effect, which is in contrast to the hitherto understanding that a fully resolved fine structure must be a prerequisite in a nonrelativistic approximation. It has been demonstrated that under certain conditions this unexpected DSP can be explained as a CI-induced effect in the final ionic state. This effect is due to the quenching of the cancellation between different multiplet components as a result of their asymmetric population by internal selection rules for diagram lines.

Experimental work at the ALS was funded by the U.S. DOE, Office of Science, BES, Divisions of Chemical, Biosciences, and Geophysical Sciences. We are thankful to J. Bozek and A. Young for their help in the measurements at the beamline. One of us, U.B., is indebted to the Deutsche Forschungsgemeinschaft (DFG) for financial support.

[1] B. Lohmann, U. Hergenhahn, and N. M. Kabachnik, J. Phys. B **26**, 3327 (1993).
[2] N. Müller, R. David, G. Snell, R. Kuntze, M. Drescher, N. Böwering, P. Stoppmanns, S. W. Yu, U. Heinzmann, J. Viefhaus, U. Hergenhahn, and U. Becker, J. Electron Spectrosc. Relat. Phenom. **72**, 187 (1995).
[3] G. Snell, M. Drescher, N. Müller, U. Heinzmann, U. Hergenhahn, J. Viefhaus, F. Heiser, U. Becker, and N. B. Brookes, Phys. Rev. Lett. **76**, 3923 (1996).
[4] G. Snell, B. Langer, M. Drescher, N. Müller, B. Zimmermann, U. Hergenhahn, J. Viefhaus, U. Heinzmann, and U. Becker, Phys. Rev. Lett. **82**, 2480 (1999).
[5] B. Lohmann, Aust. J. Phys. **52**, 397 (1999).
[6] U. Hergenhahn, G. Snell, M. Drescher, R. Schmidtke, N. Müller, U. Heinzmann, M. Wiedenhöft, and U. Becker, Phys. Rev. Lett. **82**, 5020 (1999).
[7] B. Lohmann and U. Kleiman, in *Many Particle Spectroscopy of Atoms, Molecules, Clusters, and Surfaces*, edited by J. Berakdar and J. Kirschner (Kluwer/Plenum, New York, 2001), p. 173.
[8] B. Lohmann, J. Phys. B **32**, L643 (1999).
[9] H. Klar, J. Phys. B **13**, 4741 (1980).
[10] N. M. Kabachnik, J. Phys. B **14**, L337 (1981).
[11] K. Blum, B. Lohmann, and E. Taute, J. Phys. B **19**, 3815 (1986).
[12] N. M. Kabachnik, I. P. Sazhina, I. S. Lee, and O. V. Lee, J. Phys. B **21**, 3695 (1988).
[13] M. Drescher, T. Khalil, N. Müller, S. Fritzsche, N. M. Kabachnik, and U. Heinzmann, J. Phys. B **36**, 3337 (2003).
[14] U. Kleiman, B. Lohmann, and K. Blum, J. Phys. B **32**, L219 (1999).
[15] W. Mehlhorn, in *X-ray and Inner Shell Processes*, edited by T. A. Carlson, M. O. Krause, and S. T. Manson, AIP Conf. Proc. No. 215 (AIP, New York, 1990), p. 465.
[16] W. Kronast, R. Huster, and W. Mehlhorn, Z. Phys. D: At., Mol. Clusters **2**, 285 (1986).
[17] B. Lohmann, J. Phys. B **24**, 861 (1991).
[18] I. P. Grant, B. McKenzie, P. Norrington, D. Mayers, and N. Pyper, Comput. Phys. Commun. **21**, 207 (1980).
[19] I. P. Grant, Adv. Phys. **19**, 747 (1970).
[20] H. Aksela and J. Mursu, Phys. Rev. A **54**, 2882 (1996).
[21] J. Mursu, H. Aksela, O.-P. Sairanen, A. Kivimäki, E. Nõmmiste, A. Ausmees, S. Svensson, and S. Aksela, J. Phys. B **29**, 4387 (1996).
[22] A. T. Young, J. Feng, E. Arenholz, H. A. Padmore, T. Henderson, S. Marks, E. Hoyer, R. Schlueter, J. B. Kortright, V. Martynov, C. Steier, and G. Portmann, Nucl. Instrum. Methods Phys. Res. A **467**, 549 (2001).
[23] G. C. Burnett, T. J. Monroe, and F. B. Dunnings, Rev. Sci. Instrum. **65**, 1893 (1994).
[24] G. Snell, J. Viefhaus, F. B. Dunnings, and N. Berrah, Rev. Sci. Instrum. **71**, 2608 (2000).
[25] G. Snell, U. Hergenhahn, N. Müller, M. Drescher, J. Viefhaus, U. Becker, and U. Heinzmann, Phys. Rev. A **63**, 032712 (2001).
[26] G. Snell, B. Langer, A. T. Young, and N. Berrah, Phys. Rev. A **66**, 022701 (2002).
[27] This refers to $\phi_{exp}=135°$ in our chosen coordinate frame.